Journal of Materials Chemistry B

Accepted Manuscript

ROYAL SOCIETY OF CHEMISTRY

www.rsc.org/materialsB

Journal Name

RSCPublishing

ARTICLE

Aqueous synthesis of color tunable Cu doped Zn-In-S/ZnS nanoparticles in the whole visible region for cellular imaging

Tongtong Jiang,[a] Jiangluqi Song,[a] Huijie Wang,[a] Xuecheng Ye,[a] Hao Wang,[a] Wenting Zhang,[a] Mingya Yang,[b] Ruixiang Xia,[*b] Lixin Zhu,[*b] Xiaoliang Xu[*a]

Cite this: DOI: 10.1039/x0xx00000x

Received 00th January 2012,
Accepted 00th January 2012

DOI: 10.1039/x0xx00000x

www.rsc.org/

Cu doped Zn-In-S quantum dots (CZIS QDs) were synthesized by hydrothermal method. The absorption and fluorescence peaks of CZIS QDs shifted monotonically to longer wavelengths with the increase of Cu precursor and the decrease of Zn and In precursors. The dopant emission wavelength can be easily tuned in the whole visible region ranging from 465 nm to 700 nm by changing the molar ratio of Cu/Zn/In/S. On the basis of experimental result, it was testified that the emission of CZIS QDs was the trap state emission rather than the excitonic emission. The emission mechanisms of CZIS QDs were attributed to three kinds of approaches: (i) photogenerated holes efficiently move to trap state induced by Cu defect and recombine with the electrons in energy level of sulfur vacancy; (ii) the holes in Cu trap state recombine with the electrons in surface defect state; (iii) the electrons in conduction band recombine with the holes in levels caused by Zn vacancy. After coating ZnS shell around CZIS core, the fluorescence quantum yield of CZIS QD can reach 25-35 %. CZIS/ZnS QDs conjugated with antibodies were successfully applied for labeling Hep-G2 liver cancer cells. The cytotoxicity studies revealed that the viabilities of cell incubated with different concentrations of CZIS/ZnS QDs and different times all remained at high level of more than 90 %. Hence, the CZIS/ZnS nanoparticle is a promising material as fluorescent probe for biological application.

Introduction

Semiconductor QDs have attracted great attention for their potential application in photovoltaic cell,[1] light emitting diodes (LED)[2, 3] and bioimaging field[4] due to their unique optical and electronic properties such as tunable photoluminescence (PL), narrow emission peaks and broad excitation wavelength.[5] Cd-based QDs such as CdTe, with tunable spectra in the whole visible region and higher quantum yield of light emission have attracted a lot of research interest.[6] However, many groups have proved the toxicity of Cd-based QDs, proposing that Cd ions may diffuse into the biological environment with time.[7, 8] Hence, the inherent toxicity from the heavy metal elements limits their widespread use especially in biological field.

Recently, non-toxic I−III−VI semiconductor QDs such as Cu/In/S (CIS) QDs were considered as promising alternatives to traditional Cd-based QDs. In general, the PL peak of QDs can be easily tuned by changing reaction temperature,[10] reaction time,[11] and stoichiometric ratio of their chemical components[12] due to the change of band gap relative to the size, shape or composition.[9] In I−III−VI semiconductors, there are different kinds of intrinsic defects including vacancies, interstitial atoms, and combinations of these two, which are well-known to produce deep trap states.[13] The emission mechanisms of I−III−VI semiconductor QDs are the trap state emission rather than the excitonic emission. For these QDs, the photogenerated holes move permanently to the internal trap/defect state placed within the band gap before direct recombination.[14] As is well known that the quaternary alloy chalcogenides have greater flexibility in tuning the optical properties than ternary chalcogenides.[12] The optical spectrum of Cu-In-S-Zn can be tuned from the whole visible to near-infrared region.[9, 10] In order to improve the quantum yields and enhance photostability of semiconductor nanoparticles, ZnS shell is commonly used to eliminate surface trap states that induce a suppressed nonradiative recombination process.[7, 10, 15, 16] ZnS is an ideal material as shell for coating $CuInS_2$ or ZnCuInS cores, due to its chemical stability, nontoxicity, wide bulk band gap to localize the charge carriers inside the core region, and the smaller lattice mismatch between ZnS and $CuInS_2$.[2, 7, 17, 18] Many research groups have reported about synthesizing Cu-In-S-Zn QDs with high PL quantum yields.[2, 10]

The best PL quantum yields can reach 70−80%.[2] Han et al synthesized near-infrared $CuInS_2$/ZnS QDs embedded silica beads for cancer cell imaging.[4] Chang et al synthesized Zn-Cu-In-S/ZnS core/shell QDs and studied the applications of QDs for tumor targeted bioimaging.[11] However, these QDs were usually synthesized in organic solvents, which are not appropriate for the application in the field of biology. Although, hydrophobic QDs can be transformed into hydrophilic QDs through a ligand exchange, many organic solvents in the synthetic process are harmful to environment. In addition, the ligand exchange will cause the obvious decrease of the PL quantum yields.[5] In the view of toxicity and environment protection, hydrophilic Zn-Cu-In-S QDs synthesized directly without additional phase transfer process are better for wide application in biological field. Recently, Su et al synthesized water-soluble Cu−In−S QDs stabilized with L-cysteine and 3-mercaptopropionic acid by hydrothermal approach.[19, 20] Zhu et al synthesized $CuInS_2$/ZnS QDs using Microwave-Assisted method and obtained optimal PL QYs of 24% by changing the ratio of Cu/In.[21] Until now, there are only few studies of synthesizing $CuInS_2$/ZnS QDs in aqueous phase.

To the best of our knowledge, there is no report about direct synthesis of quaternary CZIS QDs in water solution. In this paper, Cu-Zn-In-S QDs including CZIS, CZIS/ZnS and CZIS/$(ZnS)_2$ alloyed QDs were firstly synthesized in aqueous environment. CZIS/ZnS QDs were synthesized by hydrothermal method. Sodium citrate was used as stabilizing agent in the process of synthesis. CZIS nanoparticles were synthesized by adding Cu precursor, Zn precursor, In precursor and S precursor into autoclave, respectively. Then Zn precursor and S precursor were injected to in-situ grow ZnS shell. Glutathione (GSH) was used as the capping ligand, which makes the obtained QDs being functionalized with carboxyl group and amine group. The PL peak of CZIS QDs was effectively tuned from 465 nm to 700 nm by controlling the relative stoichiometries of various chemical elements. The quantum yield of CZIS/ZnS can reach 25-35% by tuning the ratio of Cu/In/Zn and coating ZnS shell. Multiple peaks (weak peak, main peak, shoulder peak) phenomena appeared during the process of tuning various chemical elements. A mechanism of the recombination process in the multiple nanocrystal was proposed to explain these phenomena. Obtained CZIS/ZnS QDs were used as fluorescent probe to label Hep-G2 liver cancers after conjugation with antibodies. The detailed experiment process was shown in Scheme 1. Furthermore, MTT assay was conducted for researching the cytotoxicity of the obtained CZIS/ZnS QDs. Various studies have clearly demonstrated that CZIS/ZnS QDs have wide prospect in fluorescent imaging field.

Experimental section

Materials

Copper (II) chloride dihydrate ($CuCl_2·2H_2O$, 99.0%), indium chloride hydrate ($InCl_3·4H_2O$, 99.9%), sodium citrate

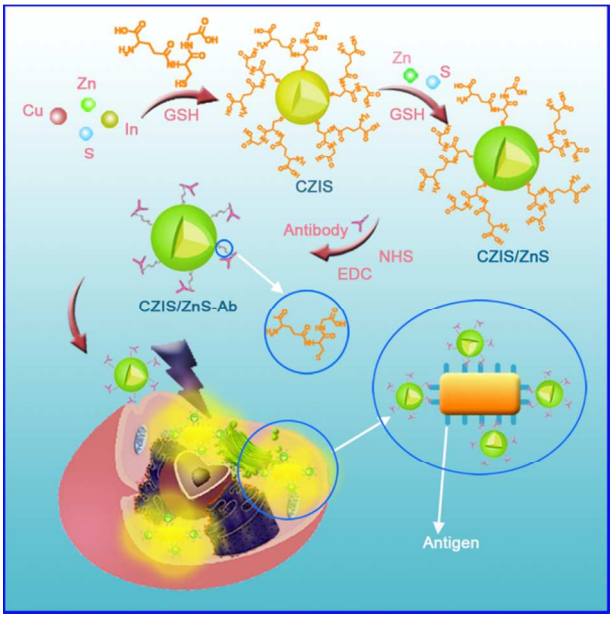

Scheme 1. Schematic illustration of the synthesis and cellular labeling process of CZIS/ZnS QDs.

($Na_3C_6H_5O_7·2H_2O$, 99.0%), zinc chloride ($ZnCl_2$, 98.0%), sodium hydroxide (NaOH, 96.0%), thiourea ($CS(NH_2)_2$, 99.0%), zinc acetate ($Zn(OAc)_2·2H_2O$, 99.0%), ethanol (99.7%) were purchased from Sinopharm Chemical Regent Co., LTD. Rabbit Anti-AFP was purchased from Beijing biosynthesis biotechnology Co., LTD. Sodium sulfide ($Na_2S·9H_2O$, 98%) was purchased from Shanghai chemical technology Co., LTD. L-glutathione (GSH), 1-ethyl-3-(3-dimethylaminopropyl) carbodiimide hydrochloride (EDC), N-hydroxysuccinimide (NHS), 4',6-diamidino-2-phenylindole (DAPI), Hep-G2 liver cancer, Cell culture media, supplements, cancer cells were all supplied by First Affiliated Hospital of Anhui Medical University. All the chemicals were used without further purification. The water used had a resistivity higher than 18.25 MΩ·cm.

Synthesis of CZIS QDs

GSH was dissolved in 25 mL of distilled water. Then $CuCl_2.2H_2O$, $InCl_3.4H_2O$, $ZnCl_2$, $Na_3C_6H_5O_7·2H_2O$ were injected into the solution. Total molar number of Cu, In and Zn sources is 0.3 mmol. The molar ratio of sodium citrate to In^{3+} and Zn^{2+} is 2:1. The pH value of the mixture solution was adjusted to 11.3 by adding NaOH (4 mol/ L). After stirring for 10 min, $CS(NH_2)_2$ was dissolved in the above solution. The double $CS(NH_2)_2$ molar number is the total of triple In^{3+} molar number and double Zn^{2+} molar number. Then the mixture solution was transferred into an autoclave and maintained at 150 °C for 23 h. The QDs were precipitated by adding ethanol to the mixture solution.

Preparation of CZIS/ZnS QDs

CZIS/ZnS QDs were prepared by adding 0.8 mmol $Zn(OAc)_2·2H_2O$, 1 mmol sodium citrate and 1.2 mmol GSH

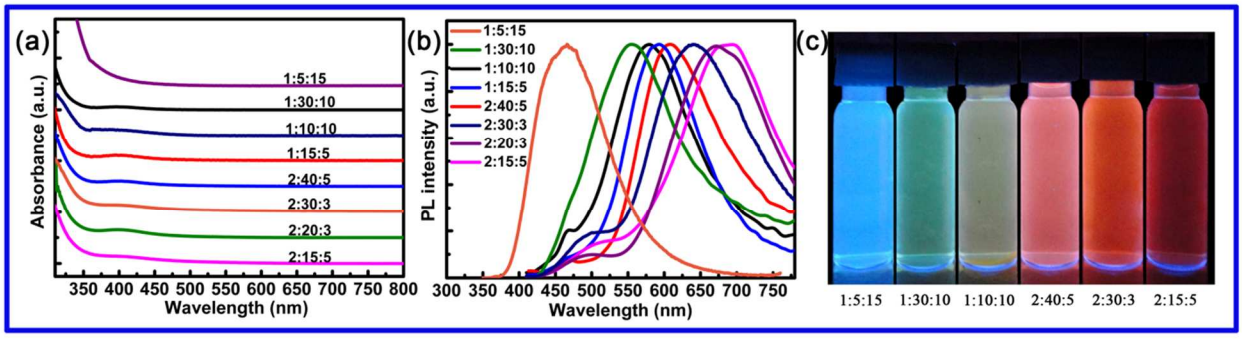

Figure 1. UV-Vis absorption spectra (a), and normalized PL spectra (b) of CZIS QDs under different Cu/In/Zn precursor ratios; the digital photograph of CZIS QDs with different Cu/In/Zn ratios under 365 nm UV light (c).

into the CZIS QDs solution. Then, 0.8 mmol Na_2S solution was slowly added. After stirring for 10 min, the reaction solution was heated for 2 h at 100 °C.

Covalent Conjugation of QDs with Antibody (Ab)

Antibodies were coupled to the surface of QDs through amide bond creation mediated by EDC and NHS. 10 mL QDs were precipitated by adding ethanol to the mixture solution and dissolved in 1 mL PBS solution. 50 μL EDC (20 mg mL^{-1}), 5 μL NHS (20 mg mL^{-1}) and 100 μL QDs were added into PBS solutions. The samples were incubated at 37 °C for 1 h in a table concentrator. 100 μL (0.1 mg mL^{-1}) of antibody was added to the PBS solution. The mixture was further incubated at 37 °C for 1 h. Finally, the product was washed with the PBS solution for further application.

Cell Culture and Cell Imaging

Hep-G2 liver cancer cells were cultured in Dulbecco's modified Eagle's medium (DMEM) containing 10 % (v/v) fetal bovine serum at 37 °C in humidified air containing 5 % CO_2. Then cells were cultured in 6-well plates in which coverslips were placed. Hep-G2 liver cancer cells were incubated for 24 h before experiments. The coverslips were carefully washed three times with PBS solution. Then PBS solution of QDs-Ab was added onto these coverslips and incubated in the humidified box for 1 h at 37 °C circumstance. Prior to imaging, the coverslips were washed three times with PBS solution. Cell images were taken by using a fluorescence microscope.

Cellular MTT Assay

Hep-G2 liver cancer cells were seeded in a 96-well microplate in complete DMEM culture medium and were incubated at 37 °C in a humidified atmosphere with 5 % CO_2 for 24 h. Then medium was discarded and different concentrations of QDs were added. Cells were incubated for different times at 37 °C with 5 % CO_2. Before 20 μL MTT stock solutions (5 mg/mL) were added to each well，wells were washed with PBS for three times and placed in a fresh DMEM solution. After 4 h incubation, 150 μL dimethyl sulfoxide (DMSO) was added to dissolve the produced formazan. Finally, the absorbance was measured using a microplate reader (ELX 800; BioTek) at 490 nm. The relative cell viability was defined as ($A_{experiment}/A_{control}$ ×100 %), where A is the absorbance.

Characterization

The morphological information of nanoparticle was obtained by transmission electronic microscopy (TEM, JEOL, JEM-2010). UV-visible absorbance and PL spectra were measured by using UV-3600 UV-VIS-NI spectrophotometer and F-4600 fluorescence spectrophotometer, respectively. Cells images were taken using Olympus IX 73 fluorescence microscope and Leica SP5 laser scanning confocal microscope. The surface chemical structure was characterized by Fourier transform infrared spectra (FTIR) spectroscopy (TENSOR27). The luminescence decay curves were measured by fluorescence lifetime spectrometer (FLS920, Edinburgh Instruments Ltd) with an excitation of 430 nm. X-ray diffraction (XRD) patterns were obtained on an X-ray diffractometer (PHILIPS Corp., X'Pert PRO). The scanning angle ranges from 20° to 70°. The chemical component was analysed by an X-ray photoelectron spectroscope (XPS) (THERMO Corp., ESCALAB250).

Results and discussion

Optical properties of the CZIS QDs

The emission and absorption properties of CZIS QDs with different Cu/Zn/In ratios were presented in Figure 1. With the change of precursor ratios, the fluorescence peak can be tuned in visible region. In the synthesis process, Zn ions were introduced to Cu-Zn-In-S QDs in two ways. In the first way, Zn ion was introduced by using $ZnCl_2$ as Zn source of synthesizing CZIS QDs. In the second way, the zinc was incorporated into QDs by coating ZnS shell around CZIS QDs, which is due to Zn interstitials at Cu vacancy sites.[10]

In order to investigate the effect of Cu, In and Zn molar ratio on the optical properties of QDs, the PL spectrum and absorption spectrum of QDs were investigated by controlling a single variable. Experimental results show that the main PL peak was blue-shifted with decreasing Cu or increasing In and

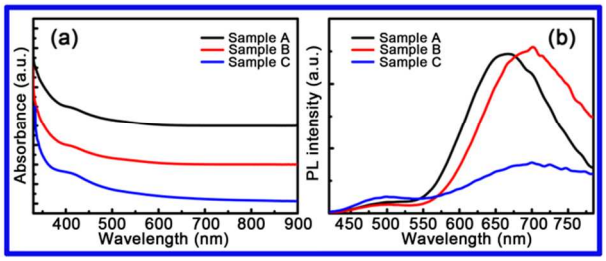

Figure 2. UV-Vis absorption spectra (a) and PL spectra (b) of CZIS QDs with different amount of S precursor. Samples A, B, C : CZIS QDs prepared under Cu/In/Zn/S precursor molar ratios of 2:20:5:70, 2:20:5:35 and 2:20:5:18, respectively.

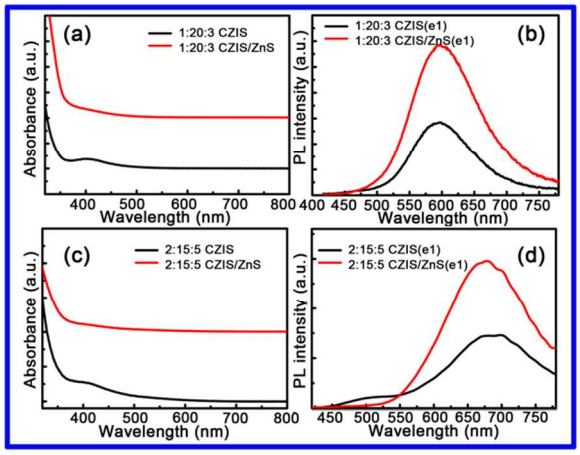

Figure 3. UV-Vis absorption spectra (a, c), PL spectra (b, d) of CZIS and CZIS/ZnS QDs, respectively.

Zn precursors. In addition, a shoulder peak around 700 nm appeared with the red shift of the main peak.(see Figure 1 b) The results clearly show that the peak position in the fluorescence spectra of CZIS QDs presented a substantial dependence on the molar ratio of Cu precursor. For further comparing the influence of Zn and In on PL peak shift, the ratio of In/Zn was increased from 1:3, 1:1 to 3:1 (Cu/In/Zn molar ratio from 1/5/15, 1/10/10 to 1/15/5), while keeping the Cu precursor and the gross amount of Zn and In precursors constant. It was found that the emission peak of CZIS was red-shifted from 463 to 591 nm.(Table S1) The phenomena demonstrate that Zn precursor ratio had greater influence on the PL peak shift of QDs than In precursor. The fluorescence peak shifted from 552 nm, 591 nm to 678 nm monotonously (Table S1) and the absorption peak shifted from 392 nm, 396 nm to 405 nm with increasing Cu/(In+Zn) ratio from 1:(30+10), 2:(30+10) to 4:(30+10), which was consistent to the previous report that the emission peak of the $CuInS_2$/ZnS QDs underwent a red shift with increasing Cu/In ratios of the precursor.[21] Corresponding Stoke shifts were 917 meV, 1033 meV and 1233 meV, respectively. Such large Stokes shift indicates that it is the trap state emission rather than a direct excitonic emission.[22]

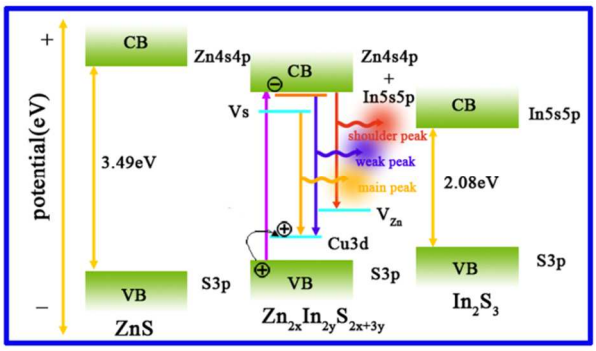

Figure 4. Schematic energy level diagram of CZIS nanoparticle.

In experimental process, an interesting phenomenon was discovered. Multiple peaks would appear in changing the relative ratio of various chemistry species. There was a weak peak around 500 nm, which had a slight shift with changing the precursor ratios. When only Cu ratio was changed, the weak and the main peak had all shifts. For investigating the effect of S element on the optical property of QDs, three samples (A, B, C) were synthesized by changing the amount of S precursor. The molar ratios of Cu/In/Zn/S in the three samples were 2:20:5:70, 2:20:5:35 and 2:20:5:18, respectively. As shown in Figure 2, only the position of the main peak had a red shift with decreasing the amount of S precursor. Figure 3a and c show the absorption spectra of CZIS and CZIS/ZnS with different Cu/In/Zn precursor ratios. The corresponding fluorescence spectra with excitation light of 400 nm (e1) were shown in Figure 3b and d, respectively. The results show that weak peaks of CZIS QDs with different precursor ratios were all suppressed after coating ZnS shell. In addition, the absorption peak around 400 nm almost disappeared, which should be due to the elimination of certain trap states on the QD surface.

In^{3+} is a hard Lewis acid, while Cu^{+} is a soft one; so they differ in their reactivity towards sulfur compounds.[23] In^{3+} and thiols have weak bonding strength. Therefore, In^{3+} has a higher reactivity than Cu^{+} ion.[24] Moreover, the introduction of Zn^{2+} complicates the whole reaction. As previously reported, Zn ion can be introduced to CIS QDs by partial cation exchange of Cu^{+} or In^{3+} with Zn^{2+}. Zn^{2+} may fill the vacancy sites related to Cu-defects.[10] Cu ions can substitute Zn ions in the Zn sites and act as acceptors. To explain these PL properties of CZIS QDs, Cu-doping hypothesis was put forward. Proposed energy diagram for CZIS were shown in Figure 4. ZnS has a wide band gap of 3.49 eV, while In_2S_3 has a band gap of 2.08 eV. The band gap of Zn-In-S should be between 3.49 eV and 2.08 eV, which consist of ZnS and In_2S_3 with appropriate ratios. For CZIS nanoparticle, Cu 3d levels will form above the edge of valence band of Zn-In-S.[25, 26] Hybridized Zn4s4p and In5s5p orbital contribute to formation of the conduction band minimum (lowest unoccupied molecular orbital (LUMO)). The valence band maximum (highest occupied molecular orbital (HOMO)) consists of S3p. Experimental results indicate that the main PL

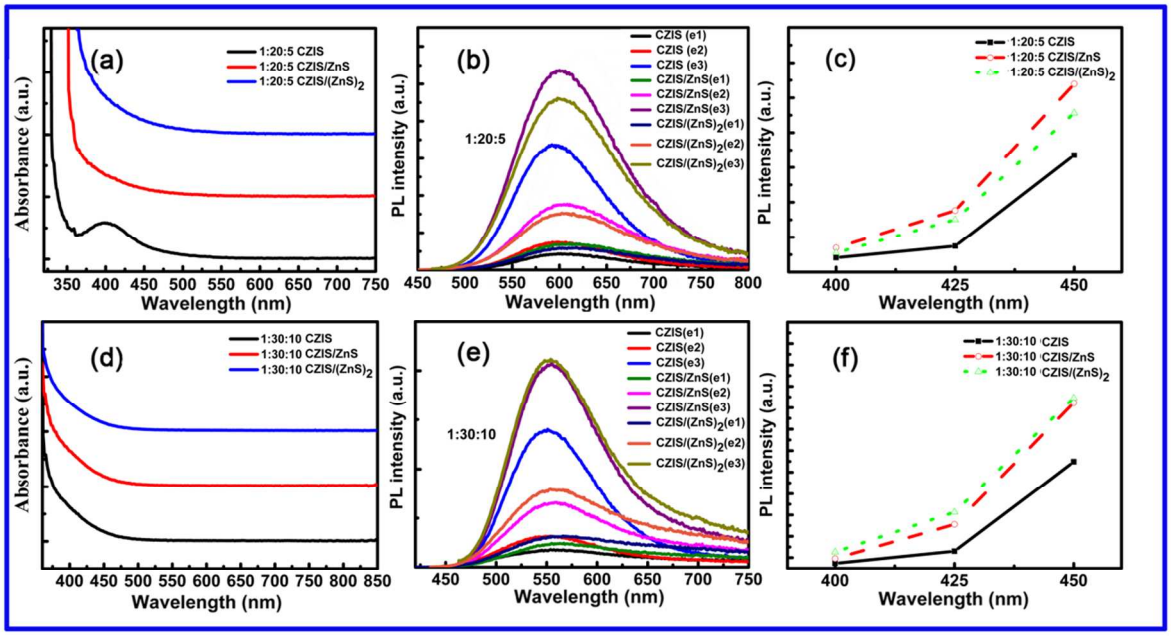

Figure 5. UV-Vis absorption spectra (a, d), PL spectra (b, e) of CZIS and CZIS with different thickness of ZnS shell, summarization of relative PL intensity and excitation wavelength (c, f). e1, e2 and e3 are the excitation wavelengths correspond to 400 nm, 425 nm and 450 nm, respectively.

peak presented clear change with varying the amount of Cu and S. Therefore, the main PL emission of CZIS QDs was attributed to the recombination between the level caused by sulfur vacancy and Cu3d level. The strong main peak should be due to great density of energy state of sulfur vacancy level. On the basis of experimental result analysis, it was proposed that the weak PL peak was due to the transfer between surface trap state and Cu3d level, which reasonably demonstrates the longer wavelength of the main peak than weak peak and the elimination of weak peak after coating a ZnS shell. When the main peak was tuned to a longer wavelength, the shoulder peak around 700 nm began to appear. Moreover, the peak didn't have any wavelength change with changing the ratio of precursors, which was ascribed to the transition between the conduction band of the host and levels caused by Zn vacancy. With the amount of Cu doped increasing, Cu 3d level would be elevated farther from the valence band,[25] causing the redshift of absorption edge and fluorescence peak (weak peak and main peak). When In or Zn precursor increased and Cu doping amount would relatively decrease, the band gap would be widen inducing the blue shift of main PL peak. With decreasing S element, Cu doping amount would relatively increase, which resulted in the decrease of the band gap. The intensity ratios of the main peak and weak peak had a slight increase with reducing S element, which should be attributed to a higher S vacancy concentration inducing a stronger main emission. But the main peak would have an obvious decrease with further decrease of S element. It may arise from less S inducing a stronger surface defect or forming other nonradiative recombination centers, and suppressing the emission of the main peak.

Figure 5 (a, b, d, e) show the UV-vis absorption and emission spectra of CZIS QDs, CZIS/ZnS, CZIS/$(ZnS)_2$ with different excitation light wavelength (e1 400 nm, e2 425 nm, and e3 450 nm). The fluorescence intensity of QDs with one layer ZnS shell had obvious improvement, which was due to the elimination of surface trap states. According to the previous report, the PL quantum yield of $CuInS_2$/ZnS QDs can reach 20-30 % by optimizing Cu/In ratio.[21] Herein, The CZIS QDs had PL quantum yield of 35 % by optimizing the Cu/In/Zn ratio (1:20:5) and coating one layer ZnS shell. The PL intensity increased or decreased slightly with the growth of ZnS shell from one layer to two layers.(see Figure 5c, f) The result should be due to that the crystal strain induced in the heterostructure increased, which caused new surface traps or crystallographic defects.[27]

Morphology and Structure of the CZIS QDs

To further understand the light emission mechanism, it is also necessary to analyze the coulomb potential energy of donor-acceptor pair (DAP) recombination, which can be expressed as following

$$U(r) = -\frac{e^2}{4\pi\varepsilon_0\varepsilon r} \qquad (1)$$

The coulomb interaction can be changed with changing the DAP separation, r. The optical energy transition condition was presented using the equation

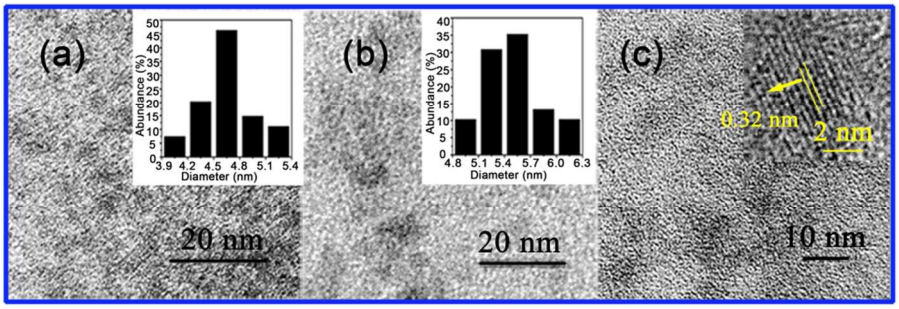

Figure 6. TEM image of the CZIS alloyed QDs with Cu:(In+Zn) ratio of 2:(30+10) (a), 4:(30+10) (b) and CZIS/ZnS QDs corresponding to Cu:(In+Zn) ratio of 4:(30+10) (c).

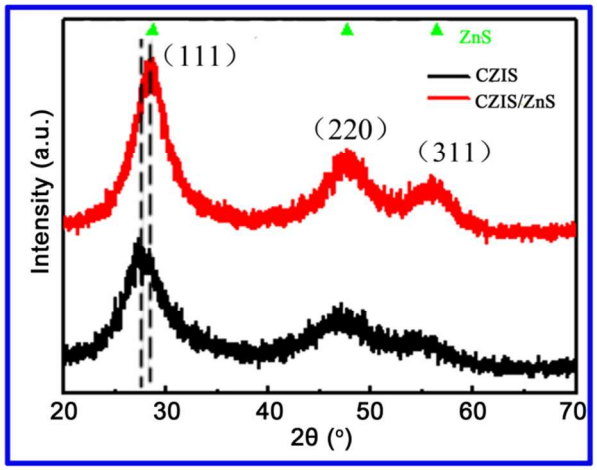

Figure 7. XRD pattern of CZIS and CZIS/ZnS QDs.

$$E_{\hbar\omega} = E_g - E_D - E_A + \frac{e^2}{4\pi\varepsilon_0\varepsilon r} \equiv \hbar\omega(\infty) + \frac{e^2}{4\pi\varepsilon_0\varepsilon r} \qquad (2)$$

where $E_{\hbar\omega}$ and E_g are the DAP recombination energy and the bulk energy band gap, respectively; E_D and E_A are the respective ionization energies of the donor and acceptor energy levels; ε is the electric permittivity; ħω(∞) is the absorption and emission energy of DAP at r = ∞. Seen from TEM images of CZIS QDs (Figure 6a, b), the diameter of CZIS changed from 4.6 ± 0.5 nm to 5.5 ± 0.5 nm with increasing the Cu doping amount. The energy shift associated with Coulomb interaction was calculated to be only ~20.3 meV when the CZIS QD size was reduced from 3.3 nm to 2.4 nm in the previous report.[28] Similarly, the energy shift associated with Coulomb interaction was ~6.35 meV when the size of CZIS QD was increased from 4.6 nm to 5.5 nm. Hence, the DAP recombination of CZIS QDs in this paper was mainly due to ħω (∞) and the Coulomb interaction between electrons and holes was ignored. The size-dependent shift of the optical band gap with the size of QDs changing from 4.6 nm to 5.5 nm was small (~ 100 meV) according to calculated size dependent optical band gaps.[29] The shift of the emission energy was 269 meV, which indicated that the PL band for QDs could be mainly attributed to a DAP recombination. Figure 6c shows the TEM image of CZIS/ZnS QDs corresponding to Cu:(In+Zn) ratio of 4:(30+10). Its high resolution transmission electron microscope (HRTEM) image was shown in the inset of Figure 6c. The lattice spacing of 0.32 nm should be attributed to the (111) planes of zinc blende. The energy dispersive spectroscopy (EDS) image of CZIS QDs testified the existence of Cu, Zn, In, S elements and the formation of CZIS nanoparticles. (Figure S1)

Figure 7 displays the XRD patterns of QDs, which consist of three major peaks. The broad diffraction peaks of CZIS and CZIS/ZnS were due to the small size of QDs. XRD pattern shows zinc-blende phase of Cu:Zn-In-S QDs, which was in good agreement with previous report.[2,30] After coating ZnS shell, the pattern of the cubic lattice was maintained.[2] Compared to the (1 1 1), (2 2 0) and (3 1 1) peaks of cubic ZnS, the three characteristic peaks of CZIS and CZIS/ZnS left shifted, which was consistent with the smaller Zn^{2+} cationic radius than those of Cu^{+} and In^{3+}.[15] The XRD pattern corresponding to CZIS /ZnS core /shell QDs slightly shifted toward the higher angels compared with CZIS QDs, which was due to the smaller lattice constant for ZnS compared with CZIS.

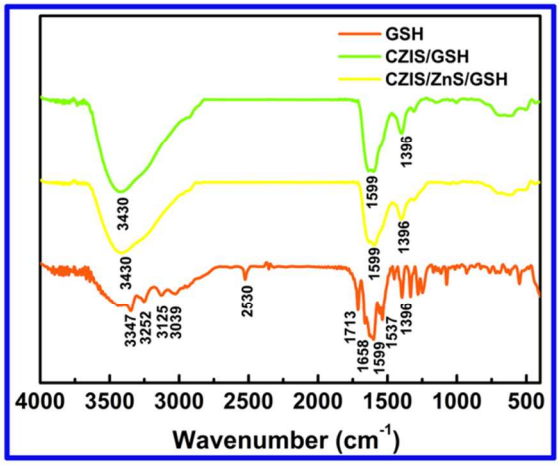

Figure 8. FTIR spectra of GSH, CZIS and CZIS/ZnS QDs.

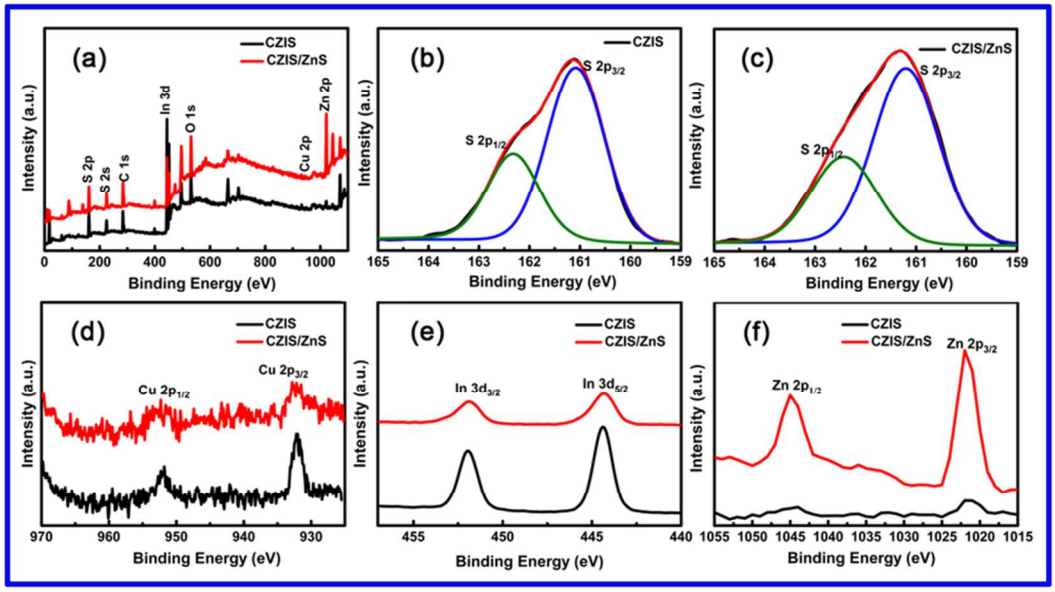

Figure 9. XPS survey spectra of CZIS, CZIS/ZnS QDs (a); XPS spectra of CZIS (b) and CZIS/ZnS QDs (c) for S 2p; and XPS spectra of CZIS and CZIS/ZnS for Cu 2p (d), In 3d (e), Zn 2p (f), respectively.

Figure 8 shows the FTIR spectra of free GSH and QDs. The peaks at 1396 cm^{-1}, 3125 cm^{-1} and 3039 cm^{-1} for GSH were due to C–O stretching and N–H stretching vibration of the zwitterion–OOC–C–NH^{3+}.[31] The peaks located at 1599 cm^{-1} and 1713 cm^{-1} were assigned to the C═O stretching band of the carboxylic group (νC═O).[32] The band at 1537 cm^{-1} and 1658 cm^{-1} were attributed to N–H deformation (amide II band) and C═O stretching vibration of the amide bond.[33] The peak at 2530 cm^{-1} was assigned to –SH. Compared with pure GSH, the disappearance of the –SH stretching vibrational peak indicated that there was a coordination between the thiol (–SH) and metal atom.[6] CZIS and CZIS/ZnS had an apparent absorption peak of -OH group at about 3430 cm^{-1} and two apparent absorption peaks of $-COO^-$ at 1599 and 1396 cm^{-1}, which indicated that CZIS and CZIS/ZnS were all functionalized with –COOH.[34]

The state of elements and composition information of CZIS and CZIS/ZnS were further determined by XPS. (Figure 9) A survey spectrum was shown in Figure 9a, indicating the presence of Cu, Zn, In and S elements. The Cu 2p core level split into Cu $2p_{3/2}$ (932.1 eV) and Cu $2p_{1/2}$ (952.2 eV), which was consistent with the literature value for Cu^+. The appearance of Cu^+ should be due to that the blue Cu^{2+} was reduced to colorless Cu^+ by thiols in an aqueous solution.[24] The peak at 444.4 eV and 452.0 eV corresponded to In $3d_{5/2}$ and $3d_{3/2}$ binding energy, indicating the chemical value state of In element was +3. The Zn core level split into Zn $2p_{3/2}$ (1021.3 eV) and Zn $2p_{1/2}$ (1044.8 eV) peaks, which was consistent with a valence of +2.[11] From S 2p core level spectrum, it can be seen that the spectrum can be divided into two peaks, which may result from the recombination of $S2p_{1/2}$ and $S2p_{3/2}$. The energy separation of $S2p_{3/2}$ and $S2p_{1/2}$ was taken constant at 1.2 eV and the relative intensities of each doublet peak was taken equal to the ratio of their respective degeneracies (2:1), in agreement with the reported data.[35] The spin split sulfur doublet peak of CZIS/ZnS underwent a red shift compared with CZIS, which indirectly indicate that ZnS shell was successfully coated onto CZIS QDs.

Table S2 shows element ratio of CZIS and CZIS/ZnS QDs as estimated by XPS. After coated by ZnS shell, it was reasonable that the ratio of Zn/S increased strongly. However, In:Cu stoichiometric ratio decreased, which should be due to that In^{3+} was gradually substituted by Zn^{2+} through an ion-exchange reaction during growth of the ZnS shell.

PL Lifetimes

The decay curves of CZIS and CZIS/ZnS were nonexponential. (Figure 10) They were fitted well with a biexponential function:

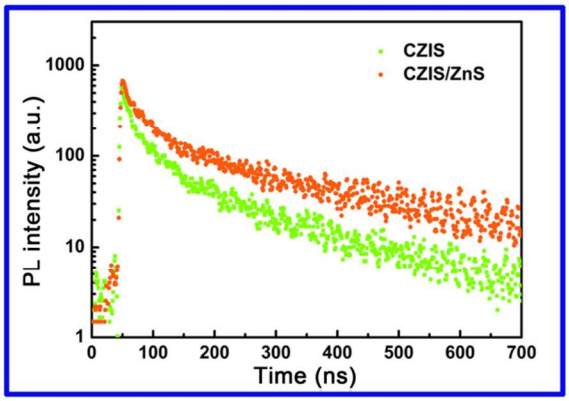

Figure 10. Time-resolved PL decay curves of the CZIS, CZIS/ZnS QDs in water.

Table 1. The fitting parameters of PL decay curves

Sample	τ_1/ns	A_1	τ_2/ns	A_2	τ_{ave}
CZIS	12.8	39.9	100.5	15.8	79.2
CZIS/ZnS	17.8	45.4	142.0	21.6	116.1

$$I(t)=I_0+A_1\exp(-t/\tau_1)+A_2\exp(-t/\tau_2) \quad (3)$$

where A_1 and A_2 are preexponential factors associated with the PL lifetimes τ_1 and τ_2, respectively. The average decay time τ was calculated by using the following equation

$$\tau=(A_1\tau_1^2+A_2\tau_2^2)/(A_1\tau_1+A_2\tau_2) \quad (4)$$

The corresponding biexponential fit parameters were presented in Table 1. The short radiation lifetime was ascribed to surface defect states. The long lifetime can be attributed to donor–acceptor pair transition.[17, 21] Surface defect states such as vacancies and dangling bonds provided local site for photoexcited electrons and holes, which had short decay lifetime compared with deep trap states.[15] Surface trap states usually occupied shallow energy level, which can be efficiently eliminated with the coating of ZnS shell. Usually, the intrinsic defects such as vacancies and interstitial atom contributed to deep trap states.[17] After the deposition of ZnS shell, the short decay lifetime τ_1 increased and $A_1/(A_1+A_2)$ decreased, indicating the reduction of surface defects. The τ_2 value and the mean decay lifetime in CZIS/ZnS core/shell QDs were greater than that of CZIS QDs, which can be attributed to the change of local environment.[15]

The stability of QDs is an important standard to measure the application prospect of these QDs. To test the stability of the as-prepared CZIS/ZnS QDs, the PL spectrum of QDs was measured after being stored for different times at room temperature and without being protected from light.(Figure S2) The PL intensities of CZIS/ZnS QDs had almost no change after being stored for sixteen days.

MTT and Cell Imaging of CZIS and CZIS/ZnS QDs

The cytotoxicity of nanoparticle is an essential measure for estimating their application prospect in biological field. In order to research the cytotoxicity of CZIS/ZnS QDs-Ab, MTT assay on Hep-G2 liver cancers with various CZIS/ZnS QDs-Ab concentrations were investigated.(Figure 11a) With increasing the concentration of CZIS/ZnS QDs-Ab from 22.5 μg/mL to 220 μg/mL, the viabilities of cells were all >90% and no obvious suppression was observed. When the incubation time increased from 2 h to 24 h, the activity of cells with the treatment of CZIS/ZnS QDs-Ab (230 μg/mL) declined by less than 10 %. (Figure 11b) However, Cell viability of control group after incubation with CdTe QDs-Ab (230 μg/mL) for 24 h had less than 15 %. Cell viability of control group incubated with CZIS QDs had also a little decline compared with that of the group incubated with CZIS/ZnS QDs. These results indicate that CZIS/ZnS QDs have an overwhelming advantage due to low cytotoxicity, which will provide a significant contribution to its prospect for the further biological labeling.

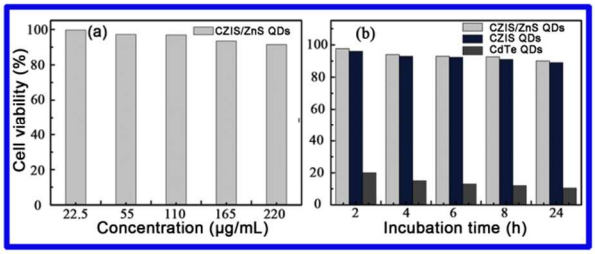

Figure 11. (a) the viability of cell incubated with CZIS/ZnS QDs-Ab of different concentration for 24 h, and (b) the viability of cell incubated with CZIS/ZnS QDs-Ab, CZIS QDs-Ab and CdTe QDs-Ab (230 μg/mL) for different times.

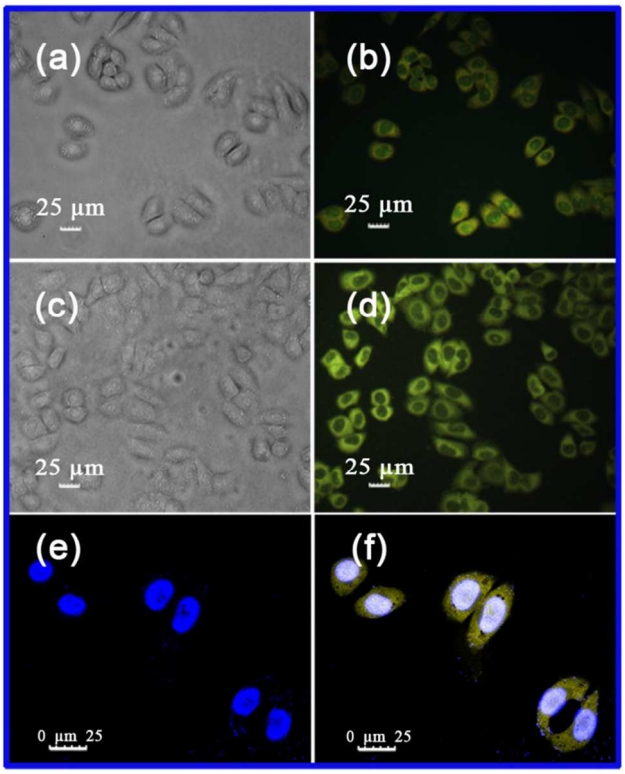

Figure 12. Bright-field image of Hep-G2 liver cancer cells after incubation with (a) CZIS QDs-Ab and (c) CZIS/ZnS QDs-Ab, (b) and (d) fluorescence image corresponding to (a) and (c) respectively. Confocal fluorescence images of Hep-G2 liver cancer cells after incubation with DAPI and CZIS/ZnS QDs-Ab taken under the conditions of (e) blue, (f) blue and yellow channel output.

To illustrate the applicability of CZIS/ZnS QDs in biological imaging, Hep-G2 liver cancer cells were labelled with CZIS/ZnS QDs-Ab. After incubation in PBS solution of QDs, the cells were washed by PBS buffer for three times. Then the cell images were taken by fluorescence microscope. The bright-field image and fluorescence image of liver cancer cells stained by CZIS QDs-Ab and CZIS/ZnS QDs-Ab were shown in Figure 12 (a, b, c, d), respectively. The morphologies of cells can be clearly observed. The cytoplasm exhibited bright yellow fluorescence under the excitation of ultraviolet light and the fluorescence intensity in the nuclei region was very weak, which was due to that QDs were abundant in the cytoplasm of

Hep-G2 liver cancer cells. It can be found that CZIS/ZnS QDs had stronger emission than CZIS QDs of the same concentration. After stained with DAPI, the liver cancer cells were observed by a laser scanning confocal microscope (Figure 12e and f). The nucleoli and cytoplasm of Hep-G2 liver cancer cells were stained by DAPI and CZIS/ZnS QDs-Ab, respectively. The fluorescence images clearly show that CZIS/ZnS QDs conjugating with Rabbit Anti-AFP can precisely target the position of cytoplasm.

Conclusions

In summary, water-soluble CZIS QDs were synthesized by using GSH as a stabilizer. With increasing concentration of Cu-doped, the absorption and emission peaks were shifted to the longer wavelength. Moreover, the PL peak underwent a blue shift by increasing the concentration of Zn (or In) precursors. The weak PL peak was attributed to the coupling of the carriers between surface trap state and Cu defect-related level. The main PL peak was predominantly due to an optical transition from energy level of sulfur vacancy to the Cu trap state. The shoulder peak was due to that the electrons in conduction band recombine with the holes in levels caused by Zn vacancy. The recombination mechanism explained the PL peak shift of CZIS QDs with different ratios of Cu, In, and Zn precursors and the elimination of the weak peak after the deposition of ZnS shell. The obtained CZIS/ZnS QDs can well label the cytoplasm of Hep-G2 liver cancer cells after conjugating with antibodies. MTT assay exhibited low cytotoxicity of CZIS/ZnS QDs, which indicates that the QDs with good biocompatibility are promising fluorescent probe.

Acknowledgements

This work was supported by the National Natural Science Foundation of China (No. 51272246 and No. 81172082)

Notes and references

a Key Laboratory of Strongly-Coupled Quantum Matter Physics, Chinese Academy of Sciences, School of Physical Sciences, University of Science and Technology of China, No. 96 Jinzhai Road, Hefei, Anhui Province, 230026, P. R. China.
b Center Laboratory, First Affiliated Hospital of Anhui Medical University, Hefei, Anhui Province, P. R. China.
Tel: +86 551 63607574;
* Corresponding Author E-mail: xrx2041@163.com, lx-zhu@163.com and xlxu@ustc.edu.cn

1 T. Torimoto, T. Kameyama, S. Kuwabata, *J. Phys. Chem. Lett.*, 2014, **5** (2), 336-347.
2 W. Zhang, Q. Lou, W. Ji, J. Zhao, X. Zhong, *Chem. Mater.*, 2014, **26** (2), 1204-1212.
3 I. S. Sohn, S. Unithrattil, W. B. Im, *ACS Appl. Mater. Inter.*, 2014, **6** (8), 5744-5748.
4 M. F. Foda, L. Huang, F. Shao, H. Y. Han, *ACS Appl. Mater. Inter.*, 2014, **6** (3), 2011-7.
5 M. D. Regulacio, K. Y. Win, S. L. Lo, S. Y. Zhang, X. H. Zhang, S. Wang, M. Y. Han and Y. G. Zheng, *Nanoscale*, 2013, **5**, 2322–2327.
6 Q. Wang, T. Fang, P. Liu, B. Deng, X. Min, X. Li, *Inorg. Chem.*, 2012, **51** (17), 9208-13.
7 G. Mandal, M. Darragh, Y. A. Wang, C. D. Heyes, *Chem. Commun.*, 2013, **49** (6), 624-6.
8 J. Y. Lee, D. Heon Nam, M. H. Oh, Y. Kim, H. S. Choi, D. Y. Jeon, C. B. Park, Y. S. Nam, *Nanotechnology*, 2014, **25** (17), 175702.
9 D. Pan, D. Weng, X. Wang, Q. Xiao, W. Chen, C. Xu, Z. Yang, Y. Lu, *Chem. Commun.*, 2009, (28), 4221-3.
10 Z. Leng, L. Huang, F. Shao, Z. Lv, T. Li, X. Gu, H. Han, *Mater. Lett.*, 2014, **119**, 100-103.
11 W. Guo, N. chen, Y. Tu, C. Dong, B. Zhang, C. Hu, J. Chang, *Theranostics*, 2013, **3** (2), 99-108.
12 H. Xu, W. Zhang, W. Jin, Y. Ding, X. Zhong, *J. Lumin.*, 2013, **135**, 47-54.
13 B. Mao, C.-H. Chuang, C. McCleese, J. Zhu, C. Burda, *J. Phys. Chem. C*, 2014, **118** (25), 13883-13889.
14 G. Manna, S. Jana, R. Bose, N. Pradhan, *J. Phys. Chem. Lett.*, 2012, **3** (18), 2528-2534.
15 B. Mao, C. -H. Chuang, F. Lu, L. Sang, J. Zhu, C. Burda, *J. Phys. Chem. C*, 2013, **117** (1), 648-656.
16 E. S. Speranskaya, N. V. Beloglazova, S. Abe, T. Aubert, P. F. Smet, D. Poelman, I. Y. Goryacheva, S. De Saeger, Z. Hens, *Langmuir*, 2014, **30** (25), 7567-75.
17 X. Tang, K. Yu, Q. Xu, E. S. G. Choo, G. K. L. Goh, J. Xue, *J. Mater. Chem.*, 2011, **21** (30), 11239.
18 J. Park and S. -W. Kim, *J. Mater. Chem.*, 2011, **21**, 3745–3750.
19 X. Gao, Z. Liu, Z. Lin, X. Su, *Analyst*, 2014, **139** (4), 831-6.
20 S. Liu, F. Shi, L. Chen, X. Su, *Microchim. Acta*, 2013, **181** (3-4), 339-345.
21 W. W. Xiong, G. H. Yang, X. C. Wu, J. J. Zhu, *ACS Appl. Mater. Inter.*, 2013, **5** (16), 8210-6.
22 W. Y. Liu, Y. Zhang, W. W. Zhai, Y. H. Wang, T. Q. Zhang, P. F. Gu, H. R. Chu, H. Z. Zhang, T. Cui, Y. D. Wang, J. Zhao, and W. W. Yu, *J. Phys. Chem. C*, 2013, **117**, 19288−19294.
23 J. Kolny-Olesiak, H. Weller, *ACS Appl. Mater. Inter.*, 2013, **5** (23), 12221-37.
24 Y. Chen, S. Li, L. Huang, D. Pan, *Nanoscale*, 2014, **6** (3), 1295-8.
25 S. H. Shen, L. Zhao, Z. H. Zhou, and L. J. Guo, *J. Phys. Chem. C*, 2008, **112**, 16148–16155.
26 F. Li, G. Chen, J. Luo, Q. Huang, Y. Luo, Q. Meng, D. Li, *Catal. Sci. Technol.*, 2013, **3** (8), 1993.
27 Z. Li, C. Dong, L. Tang, X. Zhu, H. Chen, J. Ren, *Luminescence*, 2011, **26** (6), 439-448.
28 Z. Tan, Y. Zhang, C. Xie, H. Su, J. Liu, C. Zhang, N. Dellas, S. E. Mohney, Y. Wang, J. Wang, J. Xu, *Adv. mater.*, 2011, **23** (31), 3553-8.
29 T. Omata, K. Nose, S. Otsuka-Yao-Matsuo, *J. Appl. Phys.*, 2009, **105**, 073106−073110.
30 S. J. Lei, C. Y. Wang, L. Liu, D. H. Guo, C. N. Wang, Q. L. Tang, B. C. Cheng, Y. H. Xiao, and L. Zhou, *Chem. Mater.*, 2013, **25**, 2991−2997.
31 B. K. Singh, P. Mishra, B. S. Garg, *Spectrochim. Acta A*, 2007, **67** (3-4), 719-29.

32 P. Huang, Q. Jiang, P. Yu, L. Yang, L. Mao, *ACS Appl. Mater. Inter.*, 2013, **5** (11), 5239-46.
33 R. Wei, J. Hu, T. Zhou, X. Zhou, J. Liu, J. Li, *Acta Mater.*, 2014, **66**, 163-171.
34 Y. Dong, N. Zhou, X. Lin, J. Lin, Y. Chi, G. Chen, *Chem. Mater.*, 2010, **22** (21), 5895-5899.
35 Z. X. Chen, D. Z. Li, W. J. Zhang, C. Chen, W. J. Li, M. Sun, Y. H. He, and X. Z. Fu, *Inorg. Chem.*, 2008, **47**, 9766-9772.

Cu doped Zn-In-S/ZnS QDs were synthesized for labeling cytoplasm and multiple peaks emission mechanisms of them were proposed.